Received: 28 February 2018 | Revised: 19 April 2019 | Accepted: 27 April 2019
DOI: 10.1002/sat.1313

SPECIAL ISSUE PAPER

WILEY

Assessment of spatial and temporal properties of Ka/Q band earth-space radio channel across Europe using Alphasat Aldo Paraboni payload

Spiros Ventouras[1] | Antonio Martellucci[11] | Richard Reeves[1] | Emal Rumi[1] | Fernando P. Fontan[2] | Fernando Machado[2] | Vicente Pastoriza[2] | Armando Rocha[3] | Susana Mota[3] | Flavio Jorge[3] | Athanasios D. Panagopoulos[4] | Apostolos Z. Papafragkakis[4] | Charilaos I. Kourogiorgas[4] | Ondrej Fiser[5] | Viktor Pek[5] | Petr Pesice[5] | Martin Grabner[6] | Andrej Vilhar[7] | Arsim Kelmendi[7] | Andrej Hrovat[7] | Danielle Vanhoenacker-Janvier[8] | Laurent Quibus[8] | George Goussetis[9] | Alexios Costouri[9] | James Nessel[10]

[1] STFC Rutherford Appleton Laboratory, RAL Space, Oxford, UK
[2] Escola de Enxeñaría de Telecomunicación, University of Vigo, Vigo, Spain
[3] Dep. Elect. Telec. e Informática, Instituto de Telecomunicações, Aveiro, Portugal
[4] School of Electrical and Computer Engineering, National Technical University of Athens, Athens, Greece
[5] Meteorological Department, Institute of Atmospheric Physics ASCR, Prague, Czech Republic
[6] TESTCOM, Czech Metrology Institute, Prague, Czech Republic
[7] Department of Communication Systems, Jožef Stefan Institute, Ljubljana, Slovenia
[8] ICTEAM, Université catholique de Louvain, Louvain-la-Neuve, Belgium
[9] School of Engineering and Physical Sciences, Heriot-Watt University, Edinburg, UK
[10] Antennas and Optical Communications Branch, NASA Glenn Research Center, Cleveland, OH, USA
[11] TEC-EFW, European Space Agency, ESTEC, Noordwijk, The Netherlands

Correspondence
Spiros Ventouras, STFC Rutherford Appleton Laboratory, RAL Space, Oxford, UK.
Email: spiros.ventouras@stfc.ac.uk

Summary

The upcoming migration of satellite services to higher bands, namely, the Ka- and Q/V-bands, offers many advantages in terms of bandwidth and system capacity. However, it poses challenges as propagation effects introduced by the various atmospheric phenomena are particularly pronounced in these bands and can become a serious constraint in terms of system reliability and performance. This paper presents the goals, organisation, and preliminary results of an ongoing large-scale European coordinated propagation campaign using the Alphasat Aldo Paraboni Ka/Q band signal payload on satellite, performed by a wide scientific consortium in the framework of a European Space Agency (ESA) project. The main objective of this activity is the experimental characterisation of the spatial and temporal correlation over Europe of the radio channel at Ka and Q band for future modelling activities and to collect data for development and testing of fading mitigation techniques.

KEYWORDS

Aldo Paraboni payload, Alphasat, ASALASCA, ASAPE, fade mitigation techniques, Ka band, measurement campaign, Q band, satellite communication services, slant path radio propagation

[Correction added on 28 June 2019, after first online publication: Author name is corrected from Alexios Coutsouris to Alexios Costouri.]

1 | INTRODUCTION

The increasing demand for higher data rates for the numerous services using satellite links and the congestion of the lower frequency bands (C, Ku) lead to the use of higher frequencies bands. In particular, this regards the use of Q- and V- bands for the feeder link[1] of large broadband satellite networks. This would permit accommodating on a broadband SatCom satellite a large number of beams (greater than 200) and adopting aggressive frequency reuse.[2] Furthermore, the exploitation of W-band spectrum on top of Q/V-band spectrum for feeder links in future high throughput satellite (HTS) systems could significantly reduce the cost of the ground segment.[3,4]

However, moving to Q/V band is (a) more demanding in terms of technology and (b) ultimately more prone to atmospheric propagation effects than those experienced at Ku and Ka band. Therefore, whilst the design of previous systems relied on the static allocation of a fade margin, Q/V band must rely on adaptive fade mitigation techniques (FMT; also defined more in general as propagation impairment mitigation techniques [PIMT]) such as adaptive coding and modulation (ACM), on-board reconfigurable antennas,[5] adaptive power control, site diversity,[6] smart gateway diversity,[7] and other methods.[8,9] This is an adaptive approach to system design that requires a thorough understanding of the temporal and spatial propagation characteristics of the radio channel on a large scale, including continental coverage[10-12] and more accurate predictions of propagation parameters for link budget calculations.[13]

Current propagation models are based on a number of previous propagation experiments—like OPEX with ESA OLYMPUS satellite,[14,15] CEPIT with Italian Space Agency (ASI) ITALSAT F1 satellite,[16,17] and NAPEX with NASA ACTS satellite.[18] These campaigns were complemented more in the recent years by a relevant number of Ka band campaigns using the beacons of commercial SatCom satellites (eg, EUTELSAT Hotbird 6 and Ka-Sat and ASTRA 3B).[19-21] All these campaigns provided key information for development and testing of models for distributions of propagation parameters (eg, total attenuation), second-order distributions (eg, fade and interfade durations), and a preliminary assessment of spatial–temporal channel models.

Nowadays, the experimenters can use the Ka/Q band propagation signal for scientific experiment (SCIEX[22]) transmitted by the Aldo Paraboni payload (TDP5) from the Alphasat satellite, in orbit since July 2013. This experiment permits a large-scale European campaign for the complete characterisation of the spatial-temporal channel on a continental scale. The operations of the payload must be complemented by coordination of experimenters. To this end, ESA and ASI promoted since 2014 the collaborative group of the AlphaSat Aldo Paraboni propagation Experimenters (ASAPE) to coordinate and discuss results of a number of ongoing other ESA, ASI, and National projects.

In this framework, ESA initiated in 2015 a dedicated project for a large-scale measurement campaign using the Alphasat SCIEX Ka/Q band signals (ASALASCA).

The main objective of the ASALASCA experiment is to collect a Ka/Q band experimental dataset to support the development of new or improved models for the spatial and temporal correlation of the radio channel. The statistics will also be submitted to ITU-R Study Group 3 “Radiowave Propagation” for radio regulatory activities.

The ASALASCA project is executed by a consortium including RAL Space in the United Kingdom (as prime responsible); University of Vigo in Spain; Institution of Telecommunications-Aveiro in Portugal; National Technical University of Athens (NTUA) in Greece; Universite Catholique de Louvain-la-Neuve (UCL) in Belgium. Later on, the original ASALASCA network has been augmented a) to include data from independent ESA projects, namely, the Slovenian campaign performed by Jozef Stephan Institute (JSI),[23,24] the Czech Republic Campaign performed by the Institute of Atmospheric Physics (IAP), and the Czech Metrological Institute (CMI),[25] and b) to coordinate the Q band measurements performed in Scotland by the Herriot Watt University.

The design of this campaign is based on the use of the software-defined radio (SDR) for the propagation beacon receivers and the long-term and widespread experience of experimenters on propagation data processing (derived from past ITALSAT, COST, ESA, and more recently ASAPE activities). This now makes possible to perform propagation long-term campaigns in multiple locations using a ground network of small and different terminals operated independently by each organisation in a coordinated way, collaborating at the same time with the ASAPE group. The feasibility of this approach was already demonstrated in a previous ESA activity, even using different satellites.[21]

The ASALASCA campaign also makes use of the recent development of atmospheric numerical simulators (ANSs) based on numerical weather products (NWP) to support the campaign by providing an estimate of the propagation conditions independent from beacon measurements. This approach on one hand can complement ground equipment (eg, providing an estimate of the total atmospheric attenuation to sites that are not equipped with a ground microwave radiometer), and on the other hand, it represents a test bed for the application of the ANS technology to regions where propagation data are scarce or missing.

This paper provides a description of the augmented ASALASCA experiment and its state after 2 years from the start of the campaign, together with some preliminary results. Section 2 describes the geographical and the specific technical characteristics of each experimental site. A description of the execution of the coordinated measurements, the processing of the data, and the use of numerical weather forecast simulators is given in Section 3. Section 4 shows some preliminary results, mainly to highlight the high quality of the measurements and their compliance to project requirements.

2 | EXPERIMENTAL SITES

2.1 | Geographical characteristics

The experimental campaign is based on the use of a network of ground stations in the United Kingdom (Chilbolton, Chilton, and Edinburgh), Spain (Vigo), Portugal (Aveiro), Greece (Athens and Lavrion), Czech Republic (Prague), Slovenia (Ljubljana), and Belgium (Louvain-la-Neuve). The achievable coverage is shown in Figure 1 together with the projection of the radio paths to Alphasat satellite.

The ASALASCA configuration enlarges and complements the other stations of the ASAPE group[22] and in particular fills a historical gap of measurements in the south-eastern part of Europe (where no OLYMPUS or ITALSAT data were collected).

The geographical characteristics of the experimental sites and the measured beacon signals at each site are listed in the Table 1, together with the elevation and azimuth angles. The highest and lowest elevation angles, 45.97° and 21.47°, are in Athens and Edinburgh, respectively, which are also located in rather different climatic areas.

At Aveiro, there is also a receiver to measure the beacon signal from the Ka-Sat (orbital position 9° East) at the elevation angle of 39.64° and azimuth 153.93° (see green line on Figure 1). The Ka-Sat measurements can complement the Alphasat Q band measurements for orbital diversity, interference, and in general radio channel spatial characteristics studies.

This achievable coverage area is representative of the fringe of a typical satellite covering Europe and encompassing several climatic zones (from north Atlantic to the southern Mediterranean areas), providing relevant information for model testing. Moreover, it incorporates locations in coastal zones, where the reliability of NWP data require specific evaluation.

The distances between the experimental sites are listed in Table 2. The network provides also Ka/Q band measurements at shorter scales, in Southern England and Greece, which are relevant for site diversity technique.

2.2 | Technical characteristics

The campaign is executed by a number of different terminals, operated independently by each organisation. Therefore, in this chapter, we provide a short description of the equipment of each location. This also provides an overview of the different technical design adopted by each organisation that will be useful as a reference for future campaigns.

A summary of the technical characteristics of the receiving terminals and of the measured propagation parameters is provided in Table 3. All the terminals of the network measure excess attenuation (ie, the variation of signal that can be ascribed mainly to rain attenuation) and are time synchronised (using GPS) to ensure the applicability of measurements for temporal and spatial correlation studies. Because of the specific attitude

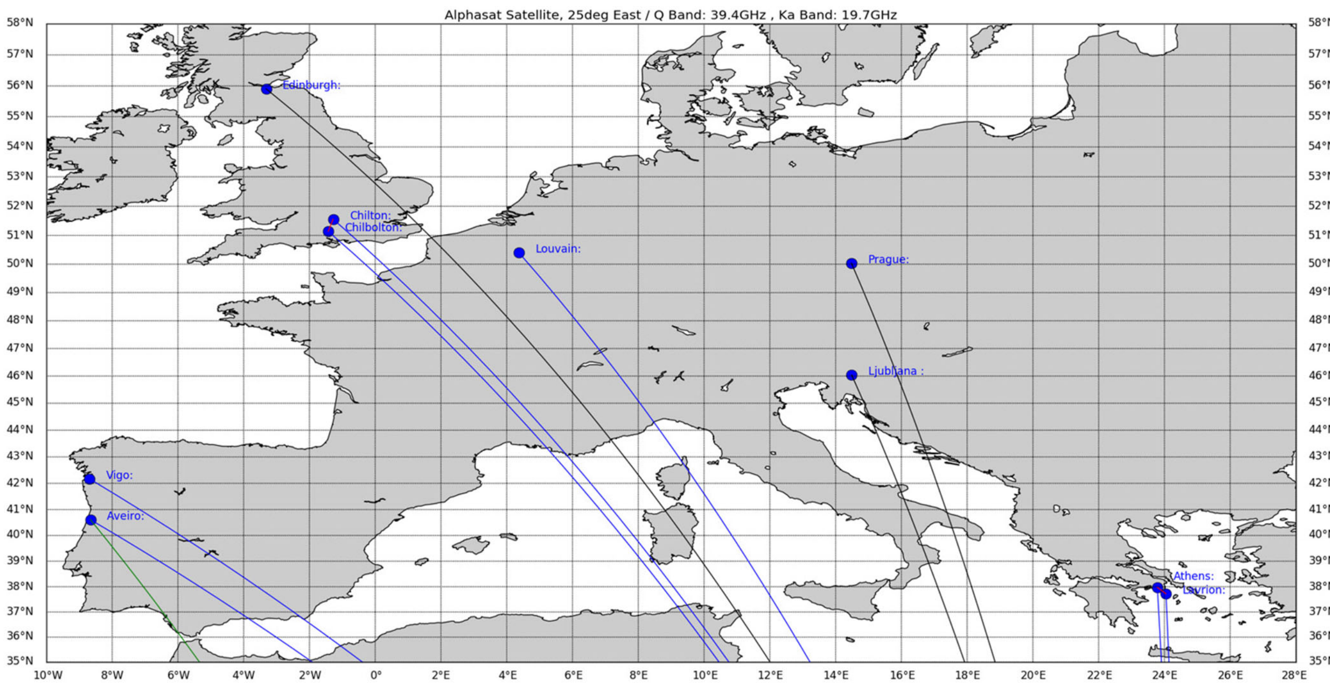

FIGURE 1 Experimental sites of ASLASCA augmented network with the projection of the radio paths to Alphasat satellite and Ka-Sat satellite [Colour figure can be viewed at wileyonlinelibrary.com]

TABLE 1 ASALASCA augmented network experimental sites information

Location	Latitude	Longitude	Above Mean Sea Level	Elevation Angle	Azimuth	Ka band	Q band
UK, Chilbolton	51.15°N	1.43°W	100 m	26.40°	147.45°	Since 11/03/2016	Since 11/03/2016
UK, Chilton	51.57°N	1.29°W	100 m	26.07°	147.77°	Since 11/03/2016	Since 11/03/2016
Portugal, Aveiro	40.612°N	8.662°W	12 m	31.80°	134.45°	KaSAT, 1/1/2013	Since 1/03/2016
Spain, Vigo	42.170°N	8.688°W	447 m	30.60°	135.20°	Since 1/1/2015	Since 1/01/2015
Belgium, Louvain-la - Neuve	50.67°N	4.61°E	160 m	29.02°	153.96°	Since 14/3/2017	Since 14/03/2017
Greece, Athens-Zografou	37.975°N	23.785°E	210 m	45.97°	178.03°	Since 1/2/2015	Since 1/07/2017
Greece, Lavrion	37.725°N	24.052°E	20 m	46.26°	178.44°	Since 1/6/2015	Since 1/07/2017
Slovenia, Ljubljana	46.042°N	14.488°E	292 m	36.0 °	165.5 °	Since 20/08/2015	Since 20/08/2015
Czech Republic, Prague	50.04°N	14.488°E	274 m	31.80 °	166.6 °	Since 01/09/2015	Since 01/09/2015
UK, Edinburg	55.91°N	3.32°W	150 m	21.47 °	146.95 °	No	Since 1/05/2016

TABLE 2 Distance in Km between experimental sites

	Chilton	Edinburg	Vigo	Aveiro	Athens	Lavrion	Louvain	Ljubljana	Prague
Chilbolton	47.9[a]	544.9	1139.6	1296.1	2456.3	2492.5	416.0	1297.2	1127.5
Chilton		502.0	1184.9	1342.3	2468.5	2504.7	415.9	1304.0	1118.2
Edinburg			1575.9	1745.1	2831.1	2867.3	798.0	1652.1	1353.3
Vigo				173.3	2784.9	2816.3	1354.5	1892.6	1977.9
Aveiro					2791.7	2821.8	1484.4	1484.4	2078.4
Athens						36.31[a]	2063.5	1179.3	1531.4
Lavrion							2099.8	1215.6	1566.7
Louvain								891.4	719.9
Ljubljana									444.5

[a]Sites for short scale radio channel spatial characterististcs, ie, site diversity.

and orbit control strategy (AOCS) of Alphasat adopted by INMARSAT, all the terminals had to be equipped with an antenna tracking system (whereas past campaigns did not need this capability). In a number of cases, the terminals are located in a temperature-controlled indoor room, behind microwave transparent windows protected against wetting due to rain. This solution permits to minimise variations of RF parameters of the front-end components that could mask atmospheric fluctuations.

Measurements of air temperature, pressure, relative humidity, wind speed and direction, and rain rate are collected at each experimental site. Chilbolton and Vigo are also equipped with a disdrometer to measure raindrop size distribution. Weather radar data and RAOBS are available at Chilbolton and Vigo stations. These data are used to support the beacon data processing and to provide information on the structure (in space and time) of key atmospheric components (eg, rain and clouds)

2.2.1 | Chilbolton and Chilton sites (UK)

RAL Space stations of Chilbolton and Chilton are equipped with identical Ka band and Q band beacon receivers and a meteorological station measuring rain rate, relative humidity, ambient temperature, and wind speed (see Figure 2). The design of RAL receivers is based on the equipment developed and tested in prior campaigns.[17,26] Detailed description of the receivers can be found in Woodroffe et al.[27]

Each of the Ka and Q band receivers uses a single downconversion to a 70-MHz IF; the signal power is measured with a Ferranti SBR100 70-MHz phase locked tracking receiver with a noise bandwidth of 30 Hz and a tracking range of ±100 kHz. The local oscillators (LOs) are dielectric resonators (DROs) phase locked to an internal crystal reference. For the Q band receivers, the LO frequency is multiplied by 3 to drive the mixer (see Figure 3).

For both sites, the two Ka and Q band receivers (and the antennas) are placed indoor where the temperature is controlled. The antennas view the satellite through radomes of woven PTFE windows (see Figure 4). The PTFE dialectic loss for both frequency bands is negligible.

Each beacon receiver is equipped with a commercial open-loop antenna tracking system (S3 SatCom Satsio Antenna System) using ephemeris TLE data provided by NORAD.[28]

TABLE 3 Characteristics of Ka and Q band terminals

	Ka band								Q band							
		Antenna								Antenna						
Exper. Site	Meas Parm.	Type	Size(mm)	Gain(dBi)	Track. system	Samp Rate(Hz)	Dyn. Range(dB)		Meas Parm.	Type	Size (mm)	Gain (dBi)	Track. system	Samp Rate (Hz)	Dyn. Range (dB)	
UK, Chilbolton	CPA, scint.	Lens horn	500	39	Yes	10	19		CPA, scint.	Cassegrain	500	44	Yes	10	22	
UK, Chilton	CPA, scint.	Lens horn	500	39	Yes	10	19		CPA, scint.	Cassegrain	500	44	Yes	10	22	
Portugal, |Aveiro	CPA, scint	Diamond shaped	1500	47	Not needed	8	24.6		CPA, scint	Cassegrain	620	45.4	Yes	8	27.5	
Spain, Vigo	CPA, scint	Lens horn	350	36	Yes	12	26.2		CPA, scint	Cassegrain	600	45.4	Yes	12	30	
Belgium, Louvain-la-Neuve	CPA, scint, XPD	Parabolic offset dish	1200	46	Yes	10	30		CPA, scint, XPD	Parabolic offset dish	1200	51.8	Yes	10	30	
Greece, Athens	CPA, scint	Parabolic offset dish	1200	46	Yes	10	39.5		CPA, scint	Shrouded parabolic	600	46	Yes	10	37	
Greece, Lavrion	CPA, scint	Parabolic offset dish	1200	46	Yes	10	36		CPA, scint	Shrouded parabolic	600	46	Yes	10	37	
Slovenia, Ljubljana	CPA, scint, XPD	Parabolic offset dish	1200	46	Yes	6.1	32		CPA, scint., XPD	Parabolic offset dish	1200	51	Yes	6.1	38	
Czech Republic Prague	CPA, scint.	Parabolic offset dish	1972 × 1822	48	Yes	1 Hz and 20 Hz	>30		CPA, scint	Parabolic offset dish	1972 × 1822	55	Yes	1 Hz and 20 Hz	>30	
UK, Edinburgh									CPA, scint	Cassegrain	600	45	Yes	10	35	

Abbreviations: CPA, copolar attenuation; scint, scintillations; XPD, cross-polar discrimination.

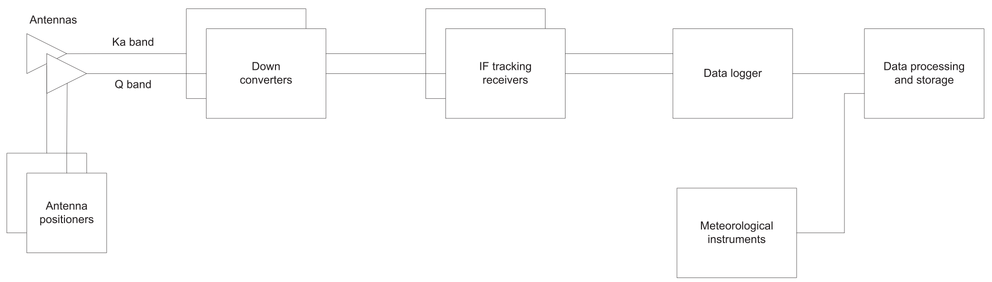

FIGURE 2 Block diagram of RAL Space terminals

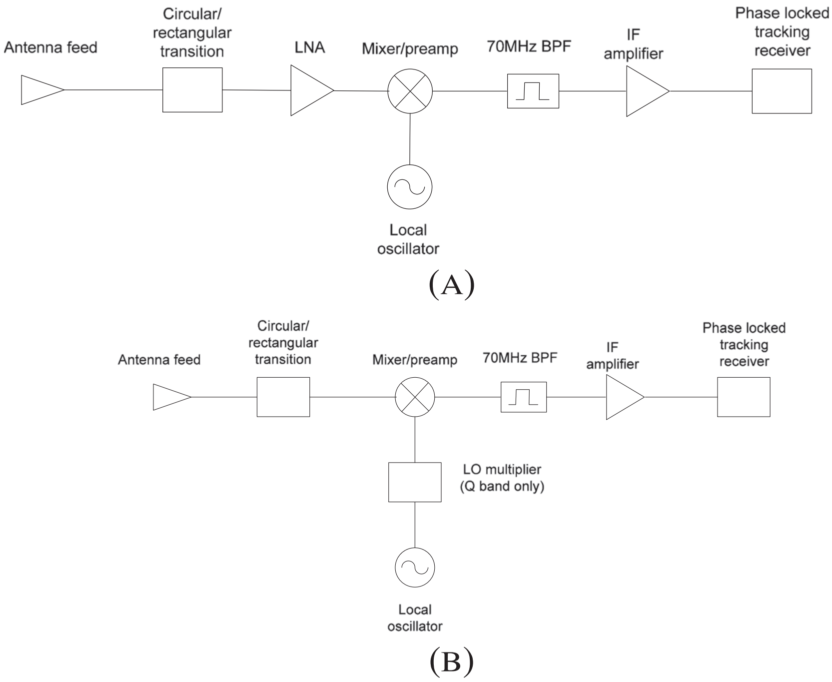

FIGURE 3 Block diagram of RAL Space receivers: A, Ka band and B, Q band

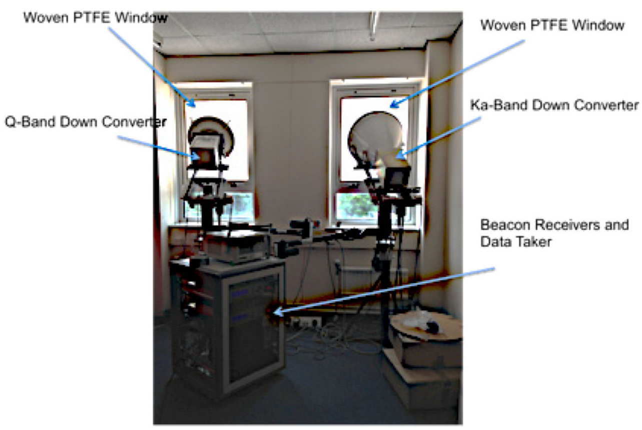

FIGURE 4 Chilton Alphasat terminals [Colour figure can be viewed at wileyonlinelibrary.com]

Rain is measured by two different rain gauges[29]: drop counting (10-s integration time, with a quantisation of 0.0033 mm of rain accumulation per drop) and tipping bucket (one tip of the bucket is equivalent to 0.2 mm of rain) measuring the number of tips per 10 seconds.[30] For this project, the drop counting rain gauge is used predominantly due to its higher sensitivity. Chilbolton site is equipped with additional instruments that could support the estimation of total atmospheric attenuation.[31]

All the time series from the beacon and meteorological instruments are stored on a daily basis at CEDA- RAL in NetCDF format.

2.2.2 | Vigo site (Spain)

The Vigo equipment consists of a dual band, single polarisation Ka and Q band beacon receiver (see Figure 5) and a co-located set of meteorological instruments: a weather station and a 2D optical disdrometer. About 60 km from the station, there is a C-band weather radar whose data are available to the experiment.[32]

The design of the Ka band RF front-end is based on the outdoor unit described in Machado et al.[33] It comprises a 35-cm diameter lens-horn antenna and a low noise block (LNB) unit. The LNB performs the low-noise amplification ($G_{LNB\text{-}Ka}$ = 55 dB and $NF_{LNB\text{-}Ka}$ = 1.3 dB) and the first frequency conversion ($IF_{1\text{-}Ka}$ = 1.451 GHz).

The Q band RF front-end has been specifically developed for the Alphasat experiment and is composed of a 60-cm diameter Q band Cassegrain antenna and a custom LNB.[32] The designed LNB consists of three main units: (a) a low noise amplifier (LNA), (b) an image rejection (IR) mixer, and (c) a phase-locked coaxial resonator oscillator (CRO) locked to a common high-stability oven controlled crystal oscillator (OCXO) reference at 10 MHz. The LNB performs the low-noise amplification ($G_{LNB\text{-}Q}$ = 20 dB and $NF_{LNB\text{-}Q}$ = 2.5 dB) and the first frequency conversion ($IF_{1\text{-}Q}$ = 142 MHz).

The receiver's data acquisition (DAQ) and signal processing have already been described in Machado et al.[32] Two ETTUS USRPs, configured in MIMO mode for synchronisation purposes, perform a second downconversion, digitise the I and Q components of both channels, decimate the signals to a rate of 200 kS/s, and send these components to a PC through a Gigabit Ethernet link (Figure 5). In the PC, a beacon receiver developed using LabVIEW SW carries out the signal acquisition, the spectral processing, and the data storage. In the default configuration, the software performs a 16384 point fast Fourier transform (FFT) to the 200-kS/s I/Q components, thus the frequency resolution (resolution band-width, RBW) would be 12 Hz, with an amplitude measurement rate of 12 S/s. Therefore, considering a Hanning window increase factor (B = 1.5) and three power-summed bins, the measurement bandwidth (MBW) of the beacon receiver would be 54 Hz. Considering these values and a 10-dB CNR margin to limit the amplitude errors, the dynamic ranges in the measurements are of approximately 26.2 dB (Ka band) and 30 dB (Q band).

Both Ka and Q band antennas are equipped with an open-loop antenna tracking system that consists of a pan-tilt unit and two digital controlled servomotors. The azimuth servomotor is coupled to the pan-tilt unit by means of a gearshift and the elevation motor is coupled by means of a ball screw linear actuator. The designed pointing system has an azimuth resolution of 0.009° and an elevation resolution of about 0.001°. The servomotors are controlled trough an RS-232 connection, using an antenna control procedure developed using LabVIEW SW. This procedure performs the regular pointing correction according to the orbit ephemeris message (OEM) files provided by ASAPE.

The dual band beacon receiver was installed in an indoor cabinet at the roof of the Telecommunications Engineering School with a 0.5-cm polycarbonate microwave transparent window, where the temperature is controlled (see Figure 6). The attenuation through the window is estimated to be less than 0.4 dB.

2.2.3 | Aveiro site (Portugal)

The Aveiro site includes the following: a co-located Ka-Sat beacon receiver at 19.68 GHz (see Rocha[34]), a meteorological station and the Alphasat Q band beacon receiver (see Figure 7).

The design of the Q band beacon receiver minimises the number of RF components and employs an SDR sampling directly the IF signal (see Figure 8). The RF hardware comprises a 62-cm diameter antenna and a low noise converter (LNC). After a low noise amplification (NF < 4 dB), with about 20 dB gain, a first downconversion is made to 2.2 GHz by using an LO derived from a PLO at 9.3 GHz and 4× frequency multiplier. After a first IF amplifier, a second and last downconversion to 142 MHz is performed using an LO at 2.06 GHz. Both LOs use a common low phase noise reference at 100 MHz. An IF amplifier delivers a signal with −52 dBm to an ELAD FDM-S2 software defined radio that performs the sampling at about 122.88 MS/s. After a digital downconversion and decimation, an I/Q data stream at 192 kS/s is delivered to a PC and stored as consecutive 100 MB wav files by the SDR Console software radio. A Matlab software on APC cyclically loads from the SDR the WAV file when ready, performs the spectral-based beacon amplitude estimation at 8 S/s, estimates also the noise spectral density, and finally, stores the estimated data

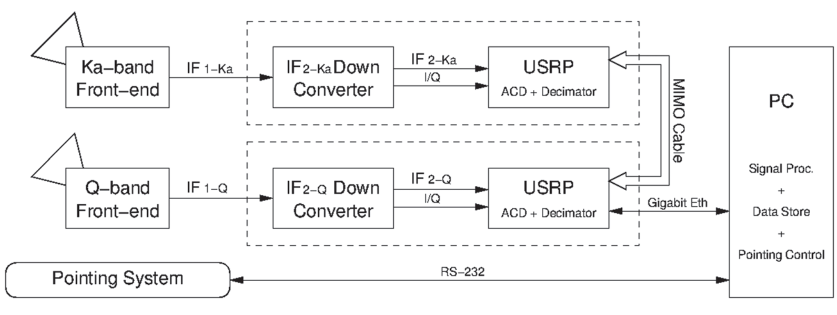

FIGURE 5 Block diagram of Vigo Alphasat dual band beacon receiver

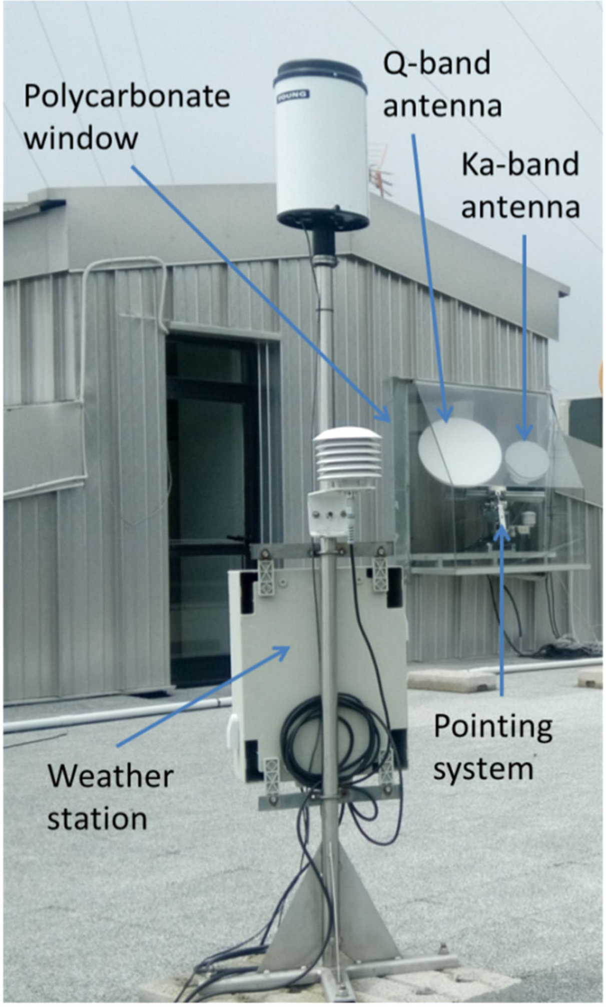

FIGURE 6 Vigo Alphasat ground station [Colour figure can be viewed at wileyonlinelibrary.com]

FIGURE 7 Aspect of indoor Q band receiver (left) and Ka-Sat receiver (right) at Aveiro [Colour figure can be viewed at wileyonlinelibrary.com]

in a processed file detected data and finally deletes the analysed WAV before restarting the cycle. The resulting MBW of this beacon receiver would be 64 Hz.

The antenna pointing system (see Figure 7) is based on a rotation/inclination axis system that is motorised by standard linear actuators fitted with optical encoders, to improve the pointing resolution to about 0.022° in each axis. A USB controller starts and stops the linear actuators according to commands from the control PC. The elevation and azimuth of the satellite are obtained from the OEM file distributed by ASAPE.

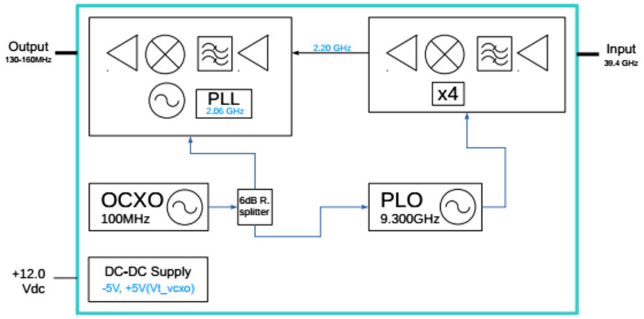

FIGURE 8 Aveiro block diagram of the Q band receiver [Colour figure can be viewed at wileyonlinelibrary.com]

The elevation and azimuth coordinates are converted to inclination and rotation coordinates and sent to the controller periodically (1 min) at each predetermined period of time. The system was calibrated against the satellite to remove any bias introduced by the mounting alignment inaccuracies and periodically verified, and its operations have been always very reliable.

The Q band receiver is installed in an indoor room with controlled temperature. The attenuation introduced by the window (see Figure 7) is estimated to be 0.4 dB at Q band.

The DAQ system of the Ka-Sat beacon receiver logs simultaneously the beacon and the meteorological channels: temperature, relative humidity, wind speed, and rain rate (both drop counter and tipping bucket rain gauges). The number of drops and tipped buckets are counted each second offering an opportunity to investigate the impact of integration time on the rain rate statistical distribution.[30]

2.2.4 | Athens and Lavrion sites (Greece)

The beacon receivers installed at NTUA Campus (Athens) and Lavrion Technological and Cultural Park (LTCP) consist of an outdoor unit (antennas, tracking systems) and an indoor/enclosed unit (including processing and system control elements) (see Figures 9, 10, and 11).

The outdoor units include (a) an offset 1.2-m dish antenna for the Ka band and (b) a 60-cm shrouded parabolic antenna for the Q band followed by LNBs and passed on to the indoor/enclosed unit. After single downconversion, the signal is brought down to an IF of 1.451 and 1.902 GHz for Ka and Q band, respectively. The downconverted signal is further filtered, amplified, and fed to Ettus USRP B210 units for signal estimation. The signals are digitised by the USRPs and are processed using a GNU Radio–based software application using an FFT-based algorithm. After running FFT on the samples, the bin with the maximum power along with three more bins in either of its sides are summed to calculate the received beacon power (using also a Blackman-Harris window to limit any spectral leakage). The FFT bin size is approx. 10 Hz. In addition, noise power is measured by averaging 1000 FFT bins at an offset of 1100 bins at either side of the beacon lobe's maximum and by multiplying the result by the equivalent beacon bandwidth (ie, 3 + 1 + 3 = 7 bins). Then resulting data are time-stamped and saved. The dynamic range for the Ka band receivers is about 40 dB for NTUA Campus and 37 dB for NTUA LTCP, whilst for the Q band ones is about 37 dB for both sites, at a data sampling rate of 10 Hz. Figure 10 depicts the receivers' simplified block diagram. The resulting MBW of this beacon receiver would be 71.72 Hz.

To get a very accurate time reference for the different receiver elements and sites, the LNB's LOs, the USRP units, and the on-board computer are all synchronised using a highly accurate GPS disciplined oscillator (GPSDO). The GPSDO feeds a 10-MHz reference signal to the LNBs and to the USRP units and a pulse per second (PPS) clock reference to align in time the received samples originating from the USRPs in time; the on-board computer runs network time protocol (NTP) in kernel GPS-PPS mode.

FIGURE 9 NTUA outdoor units at NTUA Campus, Athens (left) and NTUA LTCP, Lavrion (right) [Colour figure can be viewed at wileyonlinelibrary.com]

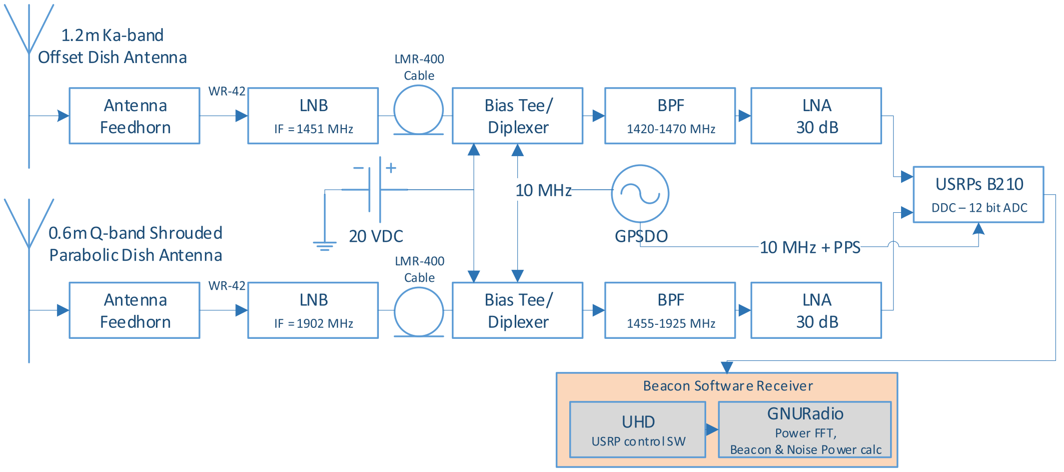

FIGURE 10 NTUA Alphasat beacon receivers simplified block diagram [Colour figure can be viewed at wileyonlinelibrary.com]

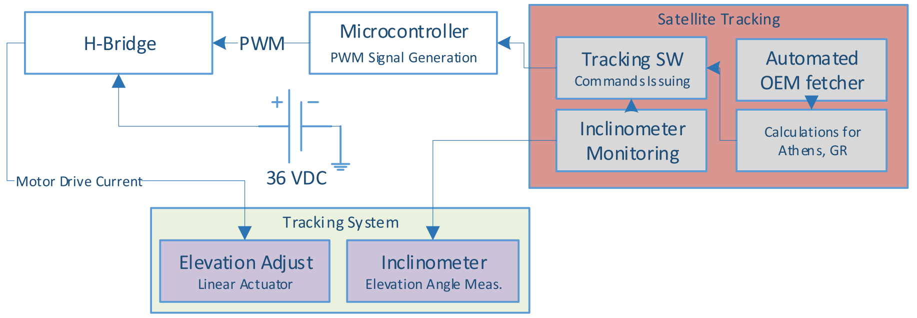

FIGURE 11 NTUA receivers tracking system simplified block diagram [Colour figure can be viewed at wileyonlinelibrary.com]

Each terminal is equipped with an antenna tracking system (see Figure 11) working only in elevation (because Athens and Lavrion are on the same longitude as Alphasat satellite position). It employs a heavy-duty linear actuator, installed together with gas springs in a push-pull configuration to dampen movement and to limit effect of wind loading. The absolute position of the antenna is measured in real-time using digital high precision inclinometers. The antenna control system is based on a scheduler that downloads OEM file distributed by ASAPE, runs the necessary calculations for each site, and issues pointing commands to the antenna tracking system. The tracking system's resolution is better than 0.05°.

Sites are equipped with meteorological sensors for temperature, humidity, wind speed and direction, atmospheric pressure, and precipitation; the precipitation is measured using tipping bucket rain gauges collocated to the receivers. The rain gauges deliver an accuracy of 0.2 mm of rain at a sampling rate of 1 Hz; each tip increases a counter recorded together with a time stamp. These data are converted to rain rate time series with 1-minute integration window.[30]

2.2.5 | Ljubljana site (Slovenia)

The beacon receiver system at JSI consists of three major subsystems, (a) the RF front-end, (b) the digital detector, and (c) the pointing system. The complete configuration is schematically depicted in Figure 12.

The RF front-end consists of a 1.2-m offset dish antenna with a custom designed 4-port feed and four LNC channels at two bands (19.7 and 39.4 GHz) and two polarisations (co-polar and cross-polar). The nominal antenna gains are 45.8 and 50.8 dBi, with half power beam widths (HPBWs) of 0.84° and 0.44°, at Ka band and Q band, respectively. A dual band/dual polarisation feed was custom designed for this specific application and the overall antenna cross-polar discrimination (XPD) is 12 and 28 dB, at Ka and Q band, respectively. To avoid losses of high frequency signal transfer, the first and the second downconversion for all four channels are performed at the outdoor unit, right after the feed. At the output, the converters provide a standard IF2 signal in the VHF range (140 MHz) led through coaxial cables to the indoor unit performing signal sampling, power estimation, and data storage.

The digital detector is implemented on a PC in a GNU radio application. It employs four universal software radio peripheral (USRP) N200 platforms with BasicRX daughter-boards, ie, one platform per channel. The same PC also runs an application to control the antenna tracking system. The signal processing at first filters the data samples with a band-pass filter. Then the samples are arranged into a vector (with 65 536 elements)

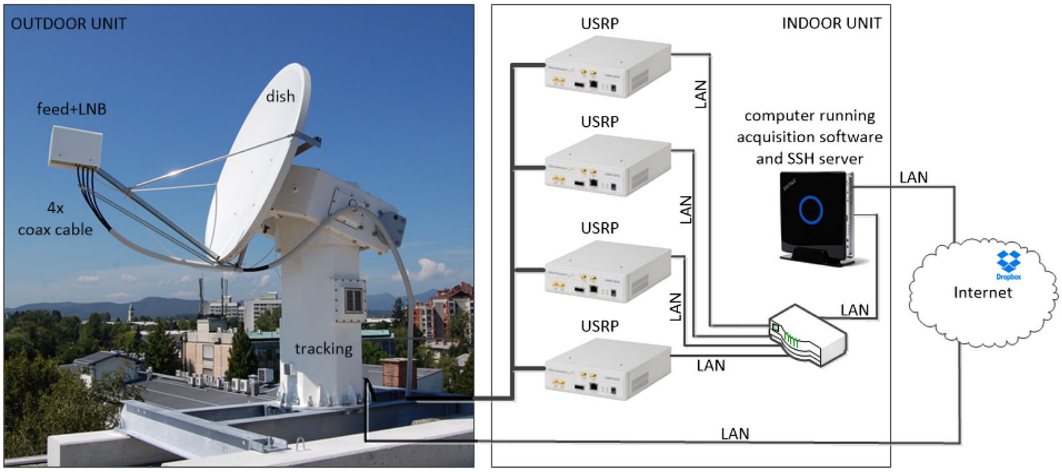

FIGURE 12 Four channel beacon receiver system at JSI in Ljubljana [Colour figure can be viewed at wileyonlinelibrary.com]

and multiplied with a flat-top window function. The vectors are converted to the frequency domain, where the signal power is estimated and recorded together with the sampling time in daily files. With a sampling rate of 400 kS/s and FFT size of 16 bit, every second, 6.1 samples of estimated power are obtained. Figure 13 shows the flow of the signal in the digital processing. The resulting MBW of this beacon receiver would be 90 Hz.

The antenna tracking system mechanism employs the two-line element (TLE) sets provided by NORAD. In addition, adaptive corrections based on received signal strength for fine-tuning are performed twice per day. The pointing resolution of the system is 0.005°.

A tipping bucket rain gauge (YOUNG 52202) is placed close to the beacon receiver and measures the number of tips per minutes and per seconds.[30] It has a collecting area of 200 cm^2, a measurement resolution of 0.1 mm, and includes a debounce circuit. The acquisition system includes also temperature and humidity sensors.

2.2.6 | Prague site (Czech Republic)

Two separate Alphasat receivers for Ka and Q bands channels (see Figure 14) are installed at this site. They are equipped with 1.8-m diameter offset parabolic antennas (Andrew Company, type 183) with electrical heating (gain: 48 and 55 dB at Ka and Q, respectively), efficiency 64%. Antenna 3-dB beam width is 0.62° and 0.32° at Ka and Q band, respectively; the antenna cross-polar discrimination is 35 and 30 dB at Ka and at Q band, respectively. The LNB is placed in the feeder at the antenna and is maintained at a constant temperature of 40°C. The LNBs downconvert the Ka and Q band signals to 1.451 and 1.702 GHz, respectively. The receivers are mounted in an outdoor rack together with power supply and communication interfaces and connected with a monitoring server via an RS485 bus using protocol Modbus.

FIGURE 13 The JSI signal processing architecture in GNU Radio

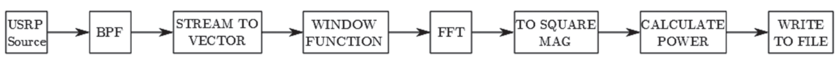

FIGURE 14 Alphasat receivers in Prague [Colour figure can be viewed at wileyonlinelibrary.com]

The IF1 is converted to an IF2 of 465 MHz (for both receivers) sent to an RSSI receiver (HopeRF chip RFM65) equipped with switchable filters (100, 10, and 1 kHz), automatic frequency control (AFC) and automatic gain control (AGC) to optimise SNR performance. The gain variation is monitored and compensated using a calibration reference. Synthesiser oscillators are controlled by an OCXO at 10 MHz. The total gain of the receiver chain is 76.7 and 76.6 dB at Ka and Q band, respectively. An extra detector is used to control the closed-loop antenna tracking system, which is performed only in elevation because of the small difference between the longitude of Prague and Alphasat orbital position. The resolution of the antenna tracking system is 0.05°. A splitter and band pass filter is also used to extract the signal at 39 GHz for an IF radiometer ("total power") channel operating on 1.7-GHz frequency to measure atmospheric noise emission with a total power radiometer.

The station is equipped with a meteorological station (WS 981 ANEMO company) measuring temperature, relative humidity, air pressure, wind speed, wind direction, and rain rate. The rain rate is measured with a tipping bucket rain gauge (resolution of 0.1 mm per tip) measuring the time of the tips.[30] A rain distrometer (JR 2D-Video 3rd generation) is installed at 100 m from the receivers. The site is also equipped with a 12-GHz "Dicke switch" type radiometer.[35]

2.2.7 | Louvain-la-Neuve site (Belgium)

The Ka/Q band Alphasat terminal is equipped with a 1.2-m offset feed antenna (Vertex/General Dynamics) with a rotation over inclination mount (span of ±10° and a dual-band, dual-polarisation feeder (LC Technologies) directly connected to the LNC block converting the Ka and Q band signals to 1.1 and 1.9 GHz, respectively (see block diagram in Figure 15).

The indoor unit contains the second converters and software defined radio receivers (ELAD FDM-S2). The detection bandwidth (MBW) of this beacon receiver is 164 Hz. The frequency reference section contains a GPS disciplined reference oscillator. As illustrated in Figure 16, the antenna positioning system contains three linear actuators controlled by the positioner/tracker controller. The controller converts the OEM files data (provided by ASAPE) into linear movements.

UCL has installed a new OTT Pluvio2 weighting rain gauge in a small meteo park located in the experimental farm, at a distance of 2 km from the receiving station, measuring the number of tips per minute.[30] The data of three pluviometers (measuring the number of tips per minute) belonging to the Walloon Region pluviometric network[30] and located at the vertices of a triangle centred on the Alphasat station are also received and processed.

2.2.8 | Edinburgh site (UK)

This site is equipped with Q band terminal. The block diagram of the front-end is shown in Figure 17. It exploits a series of mixers to downconvert the Q band signal to a 5-MHz IF frequency, which is then sampled by a DAQ card (12-bit National Instruments 5124) followed by digital processing (software defined radio). The LO of the downconverter are driven by an ultra-stable 10-MHz reference oscillator. The receiver can capture the spectrum that includes the beacon signal and implements frequency tracking of the beacon signal. A 10th order type 2 Chebyshev digital bandpass filter of bandwidth 50 kHz and measured noise bandwidth of 10.6 Hz is applied; see Figure 18B. A more detailed description of this receiver can be found in Nessel et al.[36]

The Q band antenna and RF front-end are shown in Figure 18A, where the temperatures of the LNA and RF box are monitored. The indoor computer performs data processing and logging. A weather station is also located at approximately 70 m southwards from the terminal.

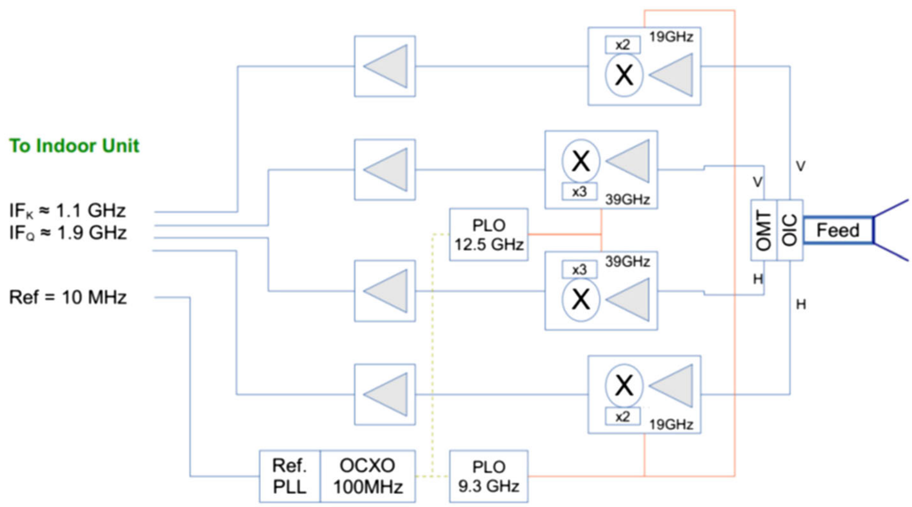

FIGURE 15 Front-end schematics of the Louvain-la-Neuve receiving station [Colour figure can be viewed at wileyonlinelibrary.com]

FIGURE 16 Aerial and antenna mount of the Louvain-la-Neuve Alphasat receiver [Colour figure can be viewed at wileyonlinelibrary.com]

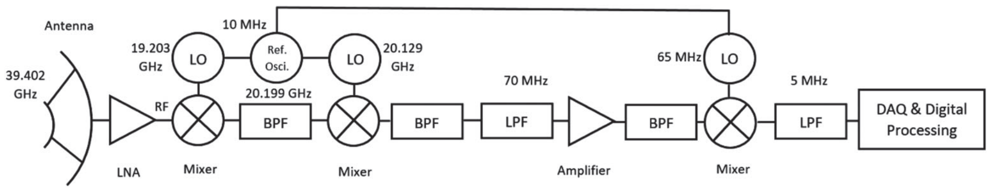

FIGURE 17 Block diagram of the downconversion to the 5-MHz IF signal and data acquisition (DAQ) card, Heriot-Watt

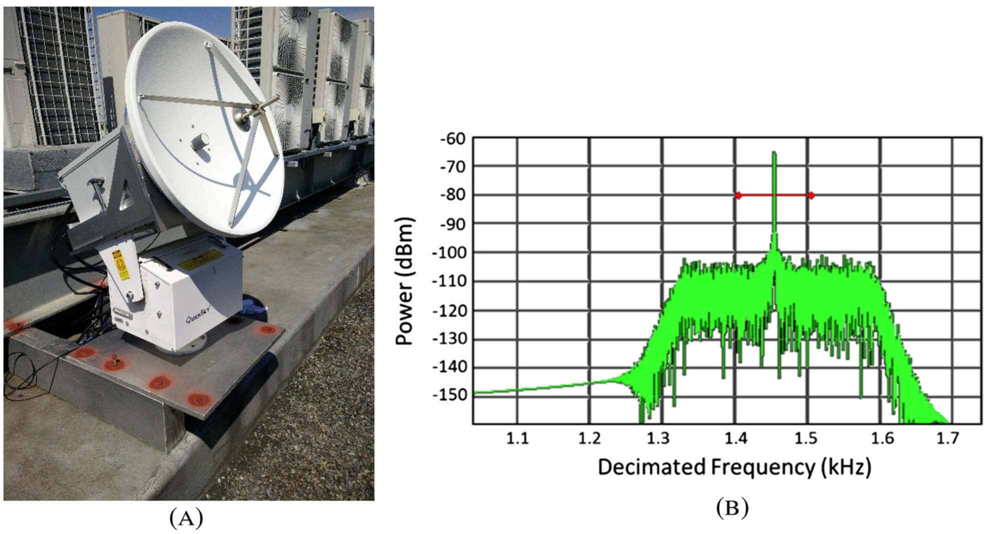

FIGURE 18 A, Photograph of the Q band beacon antenna, RF front-end box and positioner installed on the roof of the Earl Mountbatten building in Heriot-Watt University; B, image of the signal received at IF [Colour figure can be viewed at wileyonlinelibrary.com]

The terminal is equipped with an open-loop antenna tracking system (QPT 200 positioner with stepper motors) using OEM data provided by ASAPE.

3 | EXECUTION OF THE CAMPAIGN

3.1 | Organisation of experimental activities

The measurements collected by terminals, defined as level 1 (L1) raw data, are acquired and processed to generate propagation parameters (eg, excess/rain attenuation). In a first step, the effects of the space segment and ground equipment (eg, system-induced signal fluctuations and/or outliers) are removed to produce level 2 (L2) data. L2 data from different equipment (eg, beacon receiver and co-located meteorological sensors) are then merged data producing level 3 (L3) propagation data (eg, excess attenuation) according to the definitions adopted by ASAPE for data processing; see Perez et al.[37] The various data processing methods have been reviewed, compared, and preliminarily validated during the campaign design and planning phase. During the execution of the campaign, each experimenter has been responsible for the preprocessing (ie, from L1 to L3 data) of its own data, to ensure a local and continuous control of equipment performances, in particular, for the availability of L3 data. To this end, monthly reporting meetings of the consortium with ESA were held during the campaign. In addition, campaign progress reports were provided to the other experimenters during the biannual meetings of the ASAPE group.

In parallel, ANS provided statistical predictions of propagation parameters and time simulations of the radio channel conditions over the area of the ground terminals using radio-climatological data (eg, ITU-R statistical maps) and NWP concurrent data.

In the final step of the project, the L3 data will be used to perform the statistical and data analysis, producing the so-called level 4 (L4) data and the comparison with the statistical output of the ANS. At this stage, the final evaluation of the relative accuracy of the different data preprocessing algorithms will be performed, and in this case, datasets will be reprocessed. The final version of L4 data will then be submitted to ITU-R Study Group 3 for inclusion in its experimental database (DBSG3) for model testing and development.

At the moment of writing this paper, the initial planned period for the campaign has been concluded and the activities for statistical and data analysis (to derive L4 data) are starting.

3.2 | Beacon measurements and data preprocessing for monitoring

Table 1 provides the key parameters of the sites involved in the ASALASCA campaign, on which the measurements started at each site. However, the coordinated campaign started on 1 July 2016 after an initial testing phase. The ASALASCA augmented campaign started in the spring of 2017.

An overview of the different data processing methods (ie, to convert data from L1 to L3), adopted by each organisation to monitor the progress of the campaign, is described, as a reference for the statistical analysis (ie, L4 data) and for future campaigns.

All methods are based on the identification of "clear air" signal periods (ie, when there is no major rain attenuation), which are used to extract the slowly varying signal component presumably due to system effects (the so-called 0-dB reference level or clear air signal template). The excess attenuation, which should represent the rain attenuation and signal scintillation during the event, is then derived as the difference between the estimated 0-dB reference level and the measured signal level. Eventually, excess attenuation can be combined with total attenuation derived from radiometric measurements in absence of rain or from ANS data, to estimate the total attenuation due to gases, clouds, rain, and scintillation due to tropospheric turbulence. The various methods can differ in the SW implementation, interpolation methods, and level of user interaction/control.

3.2.1 | RAL method

It is based on the Fourier series expansion of the received beacon signal for both the event identification and the estimation of the clear air signal template (ie, the so-called 0-dB reference). The method was originally developed for OLYMPUS[26] and ITALSAT[17] campaigns, and it is now fully automated and implemented in Python.

This method is currently used for Chilbolton, Chilton, Athens, Lavrion, and Edinburgh data.

3.2.2 | Aveiro method

This is a complete GUI SW processing tool implemented in Matlab.[38] In this tool, data are calibrated, then possible data gaps are flagged as invalid data, and finally, time series are plotted to perform visually analysis and classification of all the channels (beacon and meteorological data).

Then clear air signal templates are derived first by plotting the beacon copolar signal levels (Ka and Q band if available) and in a separate plot an ancillary channel (usually rain rate or the noise spectral density at the Q band). Then the software automatically marks attenuation event periods (eg, with concurrent rain) that the user can manually change (eg, add/remove period of events or their start/end times). The attenuation event periods are interpolated, and FFT or polynomial techniques are used to get the clear air template (ie, the 0-dB reference level).

The template is then compared with beacon signal level, and in this case, the template can be fine "tuned" by manual interpolation with second-order polynomial or linear interpolation. The excess attenuation is derived (as the difference between the template and the signal level) and in case accepted or further processed.

This method is used for Aveiro and Vigo data.

3.2.3 | Propagation data processing system

In the frame of ESA contract,[39] a web-based propagation data processing system (PDPS) has been implemented to receive via network the L1 data from different measurement sites and to generate L3 data in a semiautomatic process. L1 data are coded using the ASAPE SPEX format[39] and are automatically processed to remove outliers, time inversions, and nonphysical values. L3 data are then automatically derived according to specific user's configuration and available ancillary data (eg, event detection can be automated thresholds on rain rate, radiometric attenuation, integrated liquid water content, or sky status index). Event detection can be corrected manually offline. Then the 0-dB reference level is derived using the days before and after the one under analysis to extract either FFT harmonics, coefficients of polynomial interpolation, or using low-pass filter. This method is used for Louvain-la-Neuve data.

3.2.4 | IAP method

The IAP method is based on FFT/IFFT and polynomial method. The most appropriate data for the 0-dB reference level is selected and combined by visual inspection, considering either clear air periods or parts of signal level during other days (up to 2 days) before and after the one under period of analysis (ie, −1 d = yesterday, −2 d, +1 d or +2 d). To avoid discontinuities between the start and the end of the templates of different periods, the FFT/IFFT is extended to cover overlap between consecutive periods (ie, from −3 h of the last day of the previous period to +3 h of the first day of the next period). This method is used for Prague data.[25]

3.2.5 | JSI method

The procedure starts with an automatic detection and removal of signal outliers. Periods of events are selected by visual inspection. During clear-sky conditions, polynomial functions are fitted to the copolar signals to derive the 0-dB reference level (see previous studies[23,40]). This method is used for JSI data.

At the beginning of the activities, an initial analysis of the data processing methods adopted by each experimenter has been done, to verify their applicability to campaign progress monitoring.

Data quality control checks are done first by the experimenter on time series and statistics and then reviewed on a monthly basis with RAL, as responsible for statistical data analysis and ESA. In case of anomalies of failures, corrective actions were discussed within the consortium, selected and executed with the objective to minimise the loss of data.

3.3 | Use of ANS for ASALASCA

The ANS was originally developed by ONERA in the framework of an ESA contract for the design of Earth Observation Ka band data downlink from non-GEO satellites.[41] It produces simulated time series and corresponding statistics of the slant path gaseous, cloud and rain attenuation for each link of the ASALASCA. The workflow of the ANS process for each site is as follows (see Figure 19):

1. Downloading meteorological data from the European Center for Medium-Range Weather Forecasts (ECMWF) 6 hours operational analysis on a 0.1° grid.
2. Running the Weather Research and Forecasting (WRF)[42] model with the ECMWF data as input. WRF covers each day of a simulation period separately, with 12 hours of spin-up. A simulation grid consists of three successive 79 × 79 domains centred on the ground station, at resolutions of 18, 6, and 2 km (see Figure 20). Vertically, there are 50 levels, up to 50 hPa (approximately 20 km). The parameterization includes the WSM6 microphysics and the Tiedtke cumulus scheme (disabled at 2 km). The output (pressure, temperature, vapour, cloud, rain) is stored every 5 minutes for the 2-km grid.

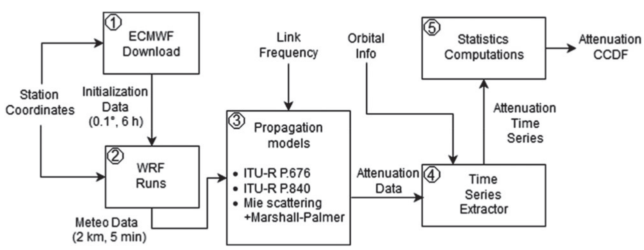

FIGURE 19 Workflow of the atmospheric numerical simulator (ANS)

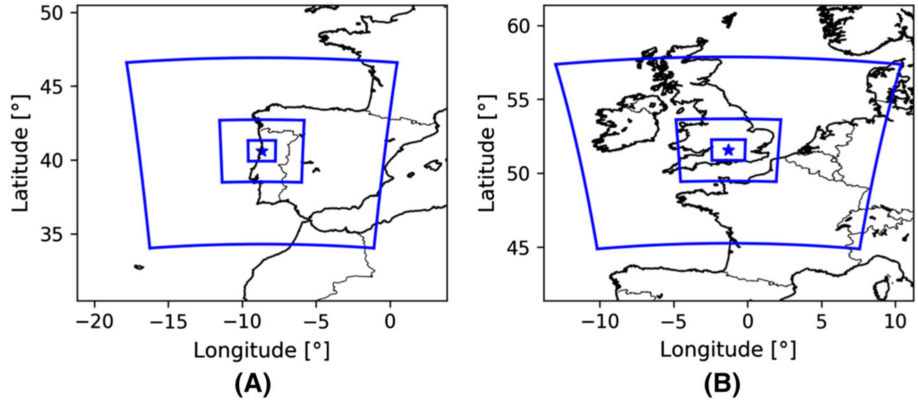

FIGURE 20 Examples of 79 × 79 Lambert Conformal Conic WRF domains at 18, 6, and 2 km used by the ANS, for Aveiro A, and Chilton B, [Colour figure can be viewed at wileyonlinelibrary.com]

3. Postprocessing the WRF 2-km grid output as in Outeiral García et al.[43] The meteorological variables are converted into specific attenuations according to ITU-R P.676-10[44] for the gases (ie, absorption lines), ITU-R P.840-6[45] (ie, Rayleigh scattering) for the clouds, and Mie scattering for the rain (assuming Marshall-Palmer distribution). Then, the specific attenuations are interpolated to an Azimuth-Elevation-Range grid. Finally, the specific attenuations are integrated to give the attenuations on an Azimuth-Elevation grid. In the case of Alphasat slant path, attenuation is calculated by using mean values of azimuth and elevation angles of the site.
4. Computing the complementary cumulated distribution functions (CCDFs) of the attenuations from the time series.

The accuracy of the ANS varies between propagation parameters. At the moment, the main conclusions are as follows:

- Gaseous and cloud attenuations are expected to be satisfactory with some underestimation of cloud attenuation with respect to radiometric measurements.[46] This could depend also on the specific methodology used in beacon data processing when dealing with cloud attenuation.

TABLE 4 Data availabilities in % of the calendar time

Site	Chilbolton		Chilton		Vigo		Aveiro		Athens	Lavrion	Ljubljana		Prague		Louvain	
Band	Ka	Q	Ka	Q	Ka	Q	Ka	Q	Ka	Ka	Ka	Q	Ka	Q	Ka	Q
July-16	79.07	99.93	99.97	99.15	89.03	89.03	99.1	99.1	81.1	87.1	97.75	97.75	100	95		
Aug-16	98.1	98.1	99.99	98.4	99.46	99.46	93.74	93.74	98.2	88	100	100	100	100		
Sep-16	99.99	99.99	82.38	82.38	99.98	99.98	99.92	99.92	98.4	84.3	100	100	100	99.2		
Oct-16	100	100	100	100	99.44	95.26	99.94	99.94	89	97.3	100	100	99.7	81.6		
Nov-16	100	100	99.99	99.99	97.56	95.52	100	100	98.2	95.9	100	100	99.9	99.9		
Dec-16	99.97	99.98	99.98	99.98	93.01	92.88	99.98	99.98	90.1	97.2	53.3	35.4	58	58		
Jan-17	100	100	100	100	99.98	99.98	100	100	72.1	76.7	91	83	16.1	16.1		
Feb-17	100	100	100	100	95.1	95.09	99.03	99.03	95.3	87.5	100	32	89.2	99.6		
Mar-17	81.16	81.17	81.05	81.16	81.34	81.34	81.24	81.24	74.7	63.5	30.5	0	44.2	49.1	38.3	38.3
Apr-17	100	100	100	100	99.98	99.98	98.44	98.44	79.6	86.4	10	10	91.4	91.4	91.6	91.6
May-17	99.59	91.11	100	100	99.98	99.98	100	100	82.5	85.8	53.2	53.2	75.3	73.6	99.9	99.9
Jun-17	100	100	100	100	99.98	99.98	100	100	92.4	100	100	100	96.5	94.2	99.9	99.9
July-17	100	100	100	99.97	99.98	99.98	100	100	74.2	87.3	100	100	100	93.2	98	98
Aug-17	100	100	100	100	99.98	99.98	99.11	99.11	99.8	100	100	100	99.9	96.7	99.9	99.9
Sep-17	97.35	97.35	97.26	97.29	99.98	99.98	100	100	92.9	100	100	100	100	99.8	99.9	99.9
Oct-17	100	100	100	100	99.98	99.98	100	100	94.4	99.5	100	100	99.9	99.8	95.8	95.8
Nov-17	100	100	96.03	96.15	99.98	99.98	100	100	98.7	98.9	96.6	96.6	100	99.8	89.9	89.9
Dec-17	100	100	99.25	100	99.98	99.98	100	100	99.3	89.7	100	100	100	99.7	96.3	99

- Rain attenuation is not well predicted on an instantaneous basis, but the estimation of intensity and occurrence of the peaks of precipitation events appear to be more accurate.[41] It is expected that there will be an acceptable statistical agreement between ANS statistics and measurements for long periods (ie, one or more years).[47] At the moment, it appears that the comparison between the ANS and measurements is more useful to improve the ANS (eg, to identify sites where the ANS configuration needs to be improved to reproduce better local conditions) rather than to improve beacon data processing.

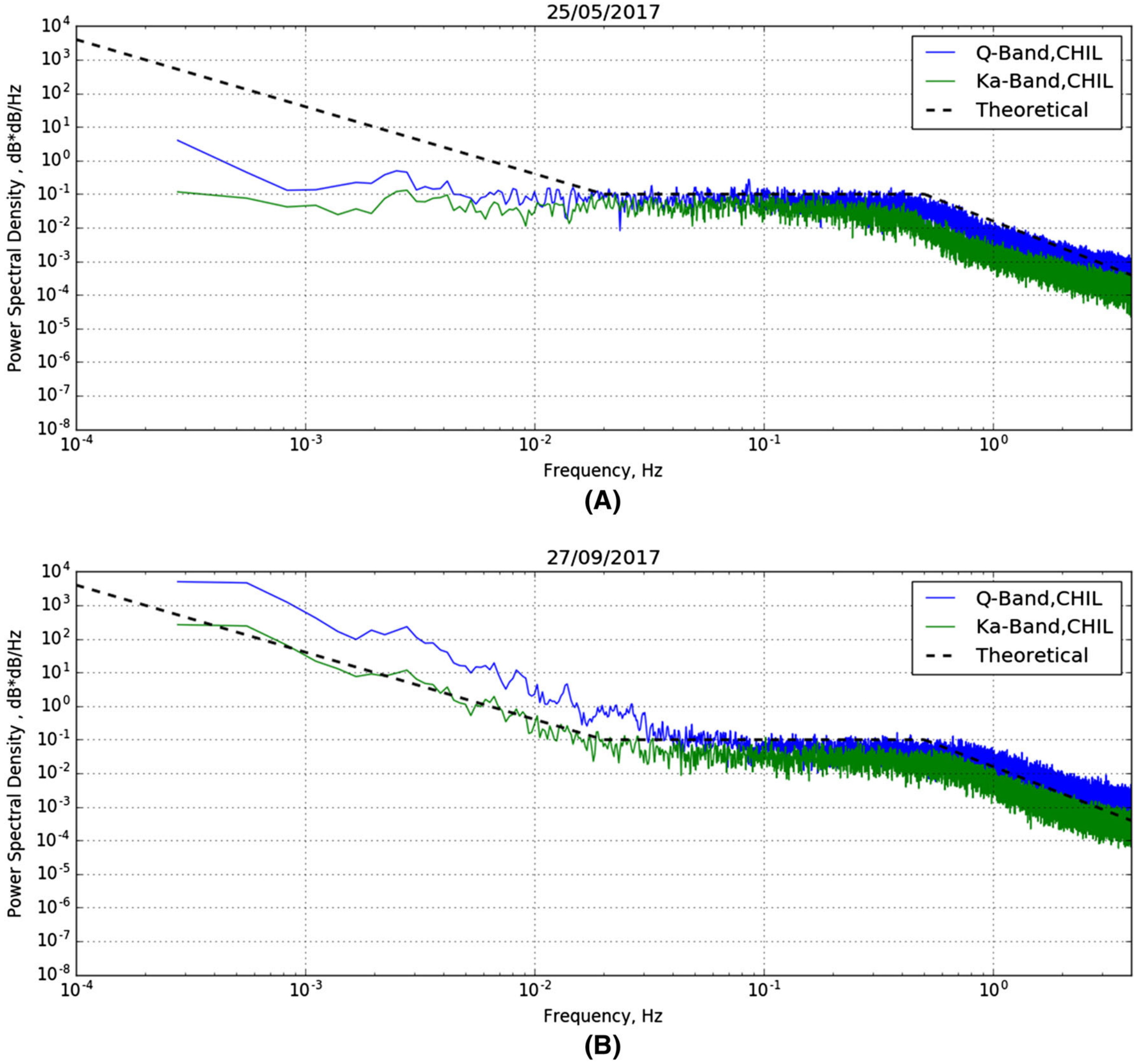

FIGURE 21 Power spectral analysis for the Ka and Q signals during a dry scintillation A, and a rain event B, Chilbolton, UK [Colour figure can be viewed at wileyonlinelibrary.com]

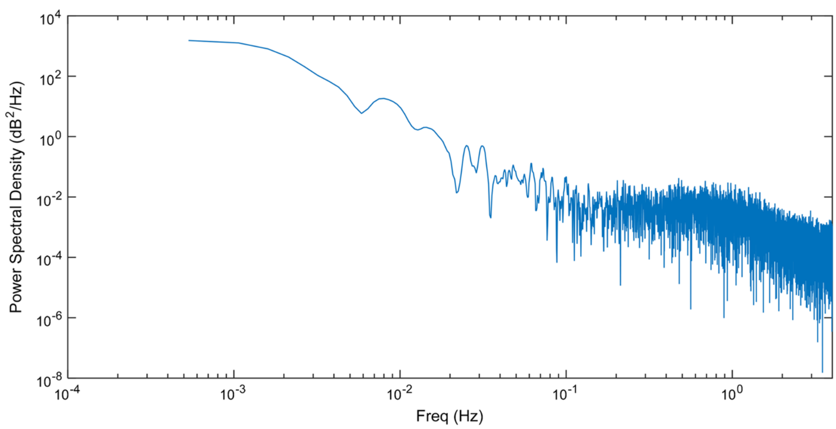

FIGURE 22 Power spectral analysis for the Q beacon during a deep attenuation event, Aveiro, March 2016, Portugal [Colour figure can be viewed at wileyonlinelibrary.com]

4 | RESULTS

This section presents some preliminary results of the campaign in 2018, before the final statistical data analysis process. The main focus is on data availability and comparability of results for different sites and applicability of ANS to data analysis.

4.1 | Beacon measurements

4.1.1 | Data availability

Table 4 lists the monthly data availability, intended as percentage of time of valid processed beacon data (Level 3) for each station of ASALASCA network and each month in the period July 2016 to December 2017. Measurements collected when attenuation exceeded the dynamic range of the receiver are still considered valid for the specific purposes of assessing statistical distributions and for correlation analyses. These data are marked as loss-lock for the calculation of second-order (ie, conditioned) distributions.

Table 4 does not include the availabilities for Edinburgh and Q band signals in Athens and Lavrion, as the processing of these data has only started recently. However, at both sites, the operational availability, intended as amount of raw data (level 1) is almost 100%. This table includes also effects of unavailability of space segment, like the planned switch off of the Alphasat Aldo Paraboni payload between 2 and 7 March 2017 during spacecraft eclipse period.

4.1.2 | Power spectral analysis

Power spectral analysis is performed on a daily basis to check the quality of the received signals, according to practice recommended by the ASAPE group. Figure 21 shows two examples of power spectral analysis of dry scintillation and a rain event in England (sampling rate 10 Hz) compared with the theoretical slopes for rain and scintillation (ie, −20 dB/decade and −80/3 dB/decade, respectively).[48] Figure 22 shows the power spectral analysis for an intense rain event in Aveiro (sampling rate 8 Hz).

4.1.3 | Geographical variability of distributions of excess attenuation

Figure 23 provides an example of the variation of the distribution of excess attenuation at Q band when passing from Southern England (Chilbolton and Chilton) to Greece (Athens and Lavrion at the other edge of the coverage area). The rain rate exceeded for the 0.01% of the average year, as predicted from the ITU-R Rec. 837-7, is around 30 and 64 mm/h for the Southern England and Athens, respectively.

4.1.4 | Spatial characteristics of the radio channel

Figure 24 shows examples of excess attenuation at Q band measured simultaneously on the same day at different sites at short (plots a and b, Chilton-Chilbolton, 47.9 km) and long distances (plots c and d, Vigo-Aveiro, 173 km) as an example of effects relevant for application of site diversity and smart gateway FMTs.

Figure 25 shows an example of the application of an ideal system switching between Chilbolton and Vigo at an attenuation threshold of 5 dB, for the same day of Figure 24. The joint signal is defined as the less attenuated signal at Vigo and Chilbolton.

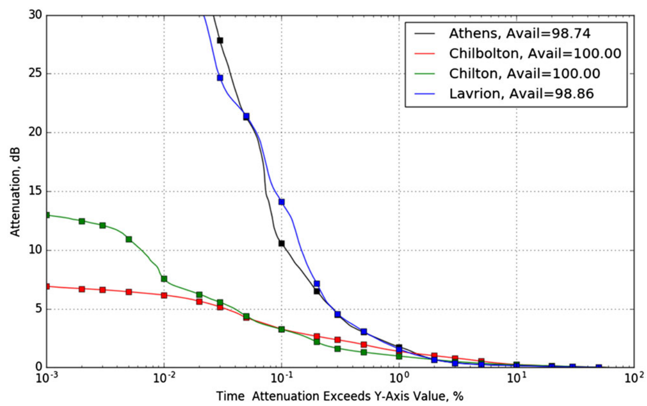

FIGURE 23 Comparison of attenuation statistics at Ka band for November 17 for Southern England and Athens [Colour figure can be viewed at wileyonlinelibrary.com]

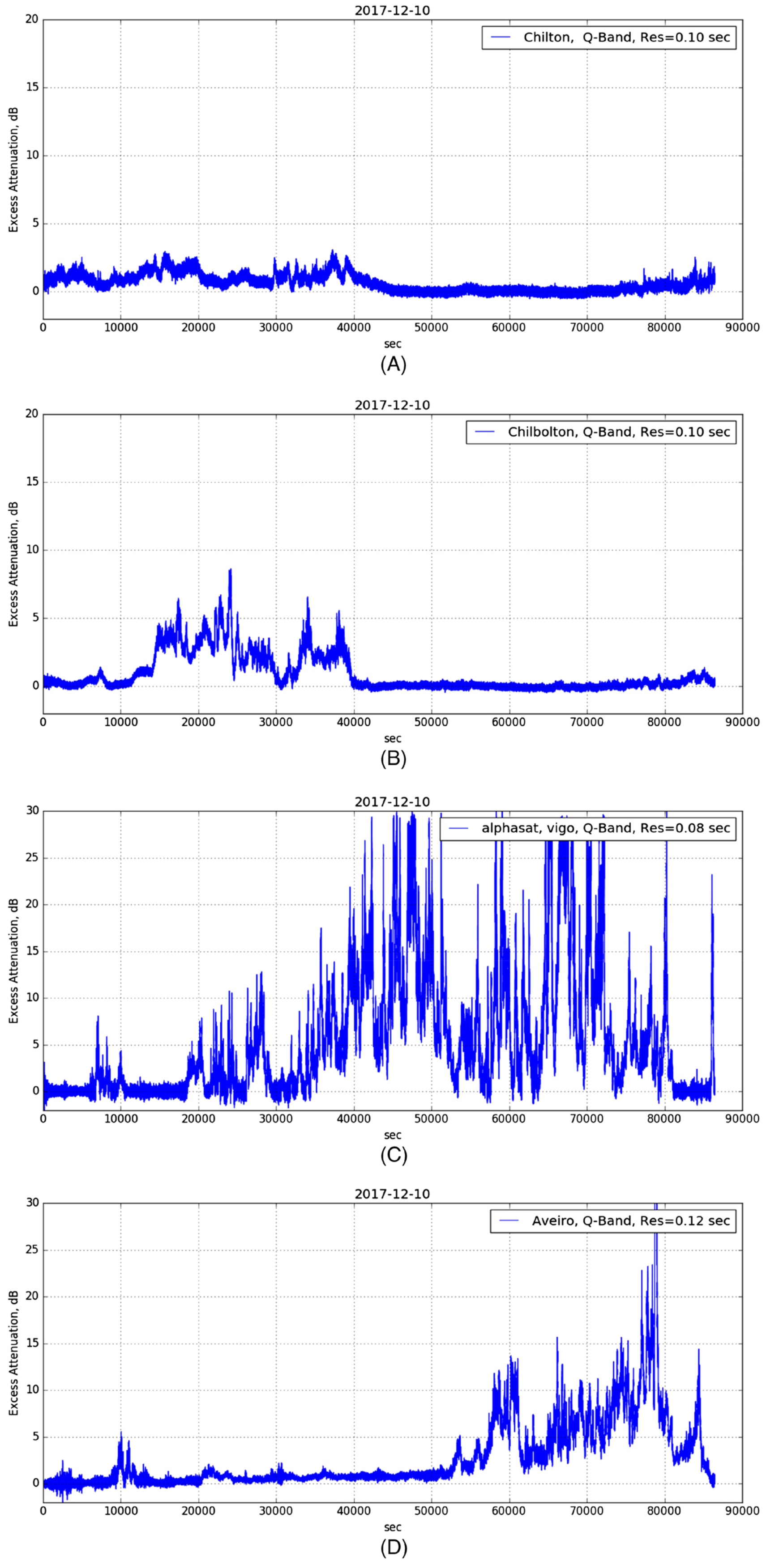

FIGURE 24 Example of the spatial characteristics of radio channel at Q band for short and large scale: Chilton A,-Chilbolton B, Vigo C,-Aveiro D [Colour figure can be viewed at wileyonlinelibrary.com]

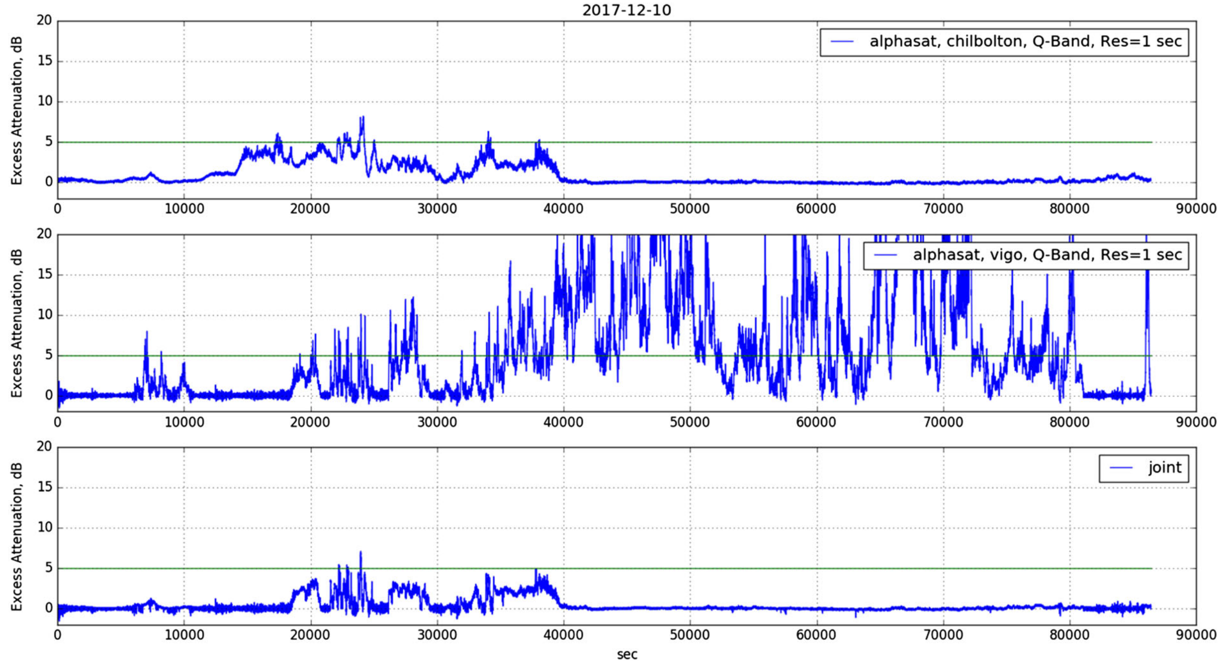

FIGURE 25 Example of the Q band joint signal (the less attenuated signal) between Chilbolton and Vigo for an ideal switching at 5 dB [Colour figure can be viewed at wileyonlinelibrary.com]

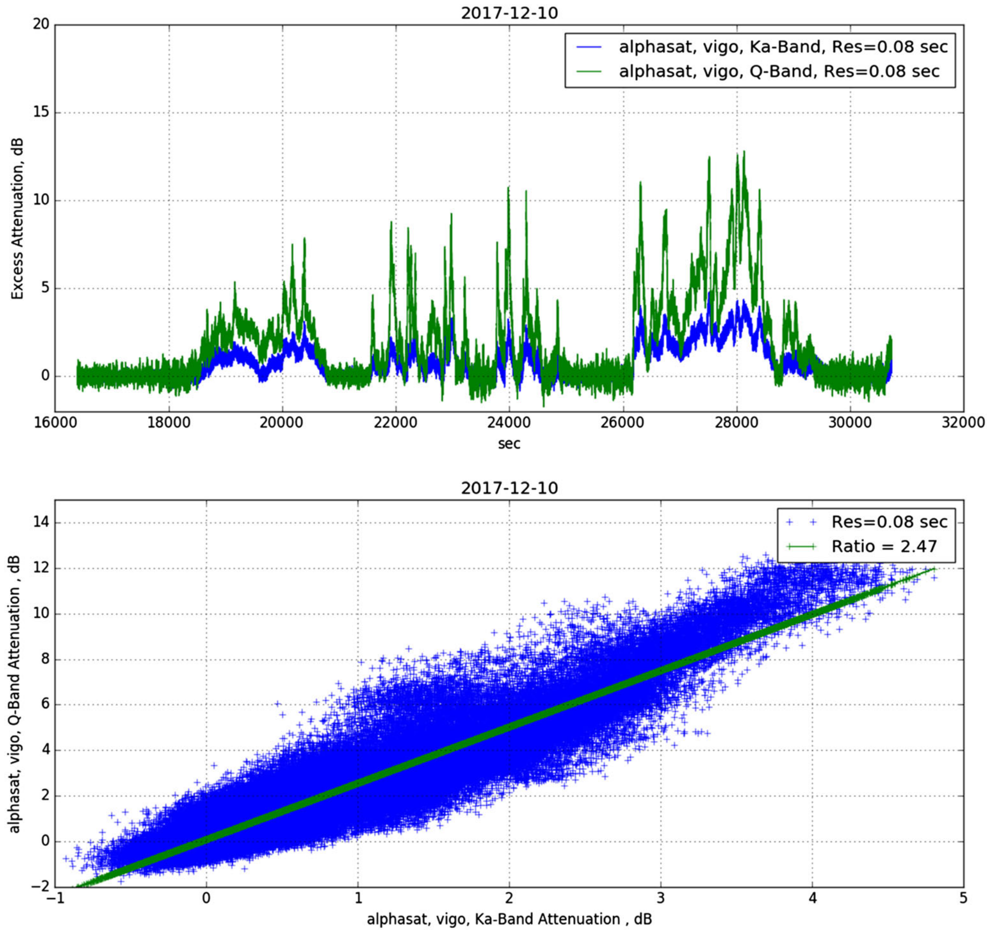

FIGURE 26 Instantaneous frequency scaling at Vigo [Colour figure can be viewed at wileyonlinelibrary.com]

Future statistical analyses will include the characterisation of the correlation coefficient and the statistical dependence index,[11] as also required by ITU-R SG3.

4.1.5 | Ka/Q band frequency scaling of excess attenuation

Figure 26 shows an example of the variability of the instantaneous frequency scaling of excess attenuation from Ka to Q band measured at Vigo on the same day of previous examples.

Figure 27 gives the distribution Q band excess attenuation conditioned to excess attenuation at Ka band derived from observations in Chilbolton from July 2016 to December 2017. The plot includes also the curve of the equiprobable values of Ka and Q band excess attenuation, which is used in comparison with the 50% decile of the conditioned distribution to detect eventual statistical data biases (see previous works[17,26]).

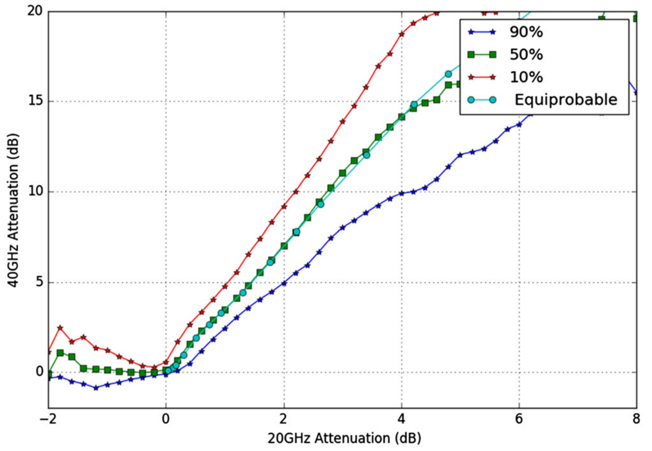

FIGURE 27 Example of the frequency scaling over the period July 2016 to Dec 2017 at Chilbolton [Colour figure can be viewed at wileyonlinelibrary.com]

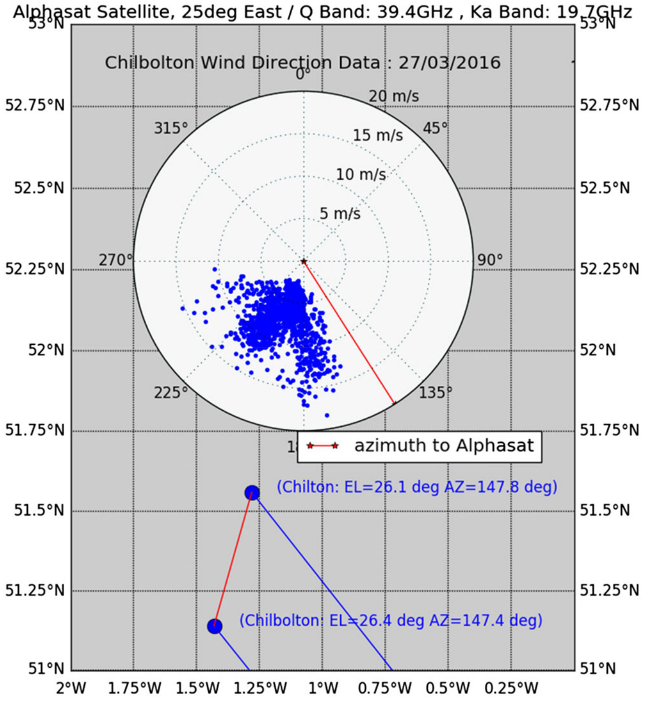

FIGURE 28 Wind speed and direction at Chilbolton [Colour figure can be viewed at wileyonlinelibrary.com]

4.1.6 | Meteo and remote sensing (ancillary) data

Figure 28 shows an example of measurements of wind speed and direction at Chilbolton in relation to baseline distance and orientation of the Alphasat link with the stations in Chilbolton and Chilton.

4.2 | Atmospheric numerical simulator

The following paragraphs provide some examples of the application of ANS results to the experimental campaign.

4.2.1 | Simulated time series of the attenuations

Figure 29 shows a 1-day time series of the different contributions to the Q band attenuation generated by the ANS for the Chilton station. The gaseous attenuation (dashed) is always present and varies slowly around 1.2 dB in agreement to previous ITALSAT observations.[17] The cloud attenuation (dashed-dotted line) gives a small contribution mostly during about the second half of the day. Rain attenuation (solid line) contributes mostly with a small peak of about 1 dB at 8 AM UTC.

The temporal resolution of ANS data is 5 minutes, which is deemed sufficient to catch the variability of gaseous (slow varying) attenuation making possible to use ANS data in clear air conditions and beacon measurements to identify the 0-dB reference level and to derive total atmospheric attenuation. In addition, the spatial and temporal resolution of the current ANS process could be sufficient to reproduce the dynamic of rain attenuation for percentages of time lower than 0.1% (see previous literature[49,50]). It still remains to be investigated the applicability of ANS data for the derivation of cloud and rain attenuation, considering that the max value of attenuation of ANS data is only limited by spatial and temporal resolution whilst VSAT class propagation terminals have a limited dynamic range.

4.2.2 | Attenuation statistics derived from the simulated time series

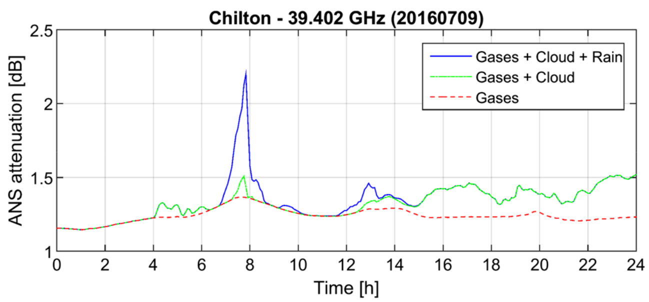

FIGURE 29 Example of attenuations time series from the ANS, for Chilton at Q band [Colour figure can be viewed at wileyonlinelibrary.com]

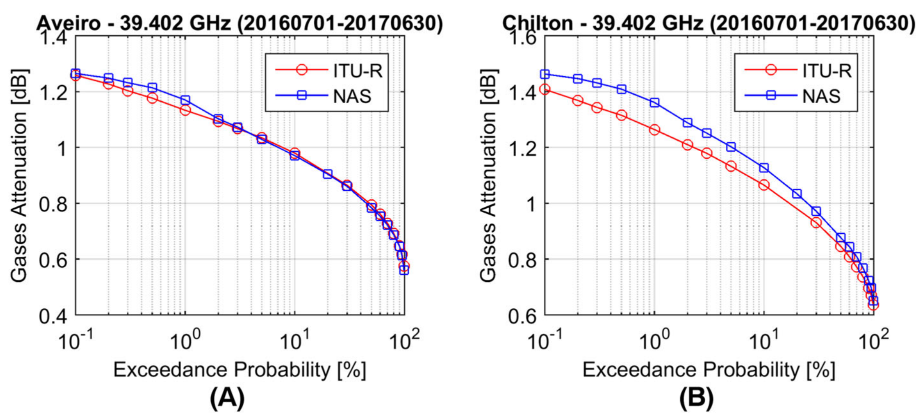

FIGURE 30 Examples of gaseous attenuation yearly CCDFs from the ANS and comparison with the ITU-R references, for Aveiro A, and Chilton B, at Q band [Colour figure can be viewed at wileyonlinelibrary.com]

Figure 30 shows statistics for the gaseous attenuation produced by the ANS over a 12-month period compared with the yearly ITU-R prediction. An agreement well within 0.1 dB can be expected based on the observed results. In the absence of independent measurements of clear-sky attenuation, this value is assumed to be indicative of the accuracy of gaseous attenuation estimated by the ANS.

5 | CONCLUSIONS

The Aldo Paraboni payload permits the extension of the results of previous campaigns (like OLYMPUS, ITALSAT, and other Ka band campaigns in more recent periods) towards the modelling of the spatial and temporal correlation of the SatCom radio channel over Europe.

To achieve this objective, ESA with a consortium of several organisations started the ASALASCA campaign in 2016 with a core network of six locations. In 2017, the network was augmented to include up to 10 locations covering Europe from in longitude Portugal to Greece and in latitude up to Scotland. Thanks to the high data availability of processed (L3) data for most of the observation period and in most of locations, it can be concluded that the main objective of collecting concurrent Ka/Q band propagation data over Europe for radio channel modelling has been achieved.

The current results of ASALASCA data processing confirm also the feasibility and the quality of coordinated propagation campaign, in which a number of scientific organisations perform measurements using their own instruments and data processing methods within the cooperative framework set by the ASAPE group.

The ASALASCA campaign has been also used to test and use new technologies and developments, including the use of SDR based for propagation terminal and the utilisation of NWP and ANS data together with local meteorological sensors to improve the understanding of the physical basis of propagation impairments, which is necessary for the development of robust prediction methodologies.

Future activities of the ASALASCA consortium will include fine tuning of data processing and statistical data analysis for the inputs to ITU-R Study Group 3 “Radiowave Propagation” for model development and testing.

ACKNOWLEDGEMENT

This work is funded by ESA Contract “Large Scale Assessment of Ka/Q Band Atmospheric Channel using the Alphasat TDP5 Propagation Beacon”, ESA-PECS project SatProSi-Alpha, ESA project—see Nessel et al.[36]

ORCID

Spiros Ventouras https://orcid.org/0000-0001-7766-1593
Armando Rocha https://orcid.org/0000-0002-5936-3020
Athanasios D. Panagopoulos https://orcid.org/0000-0003-4716-3328
Andrej Hrovat https://orcid.org/0000-0001-5220-875X
Alexios Costouri https://orcid.org/0000-0001-7687-3324

REFERENCES

1. Panagopoulos AD, Arapoglou P-DM, Cottis PG. Satellite communications at Ku, Ka and V bands: propagation impairments and mitigation techniques. *IEEE Commun Surv Tutorials*. 2004;6(3):2-14.
2. Aloisio M, Angeletti P, Coromina F, Gaudenzi R. Exploitation of Q/V-band for future braodband telecommunication satellites. Vacuum Electronics Conference (IVEC), IEEE Thirteenth International. 2012:351–352. https://doi.org/10.1109/IVEC.2012.6262191.
3. Ginesi A, Arapoglou PD. A system view for the exploitation of W-Band in future SATACOM networks. *1st ESA W Band Satcom Workshop, ESA/ESTEC*, 8 April 2015, Noordwijk.
4. Arapoglou PD. Extremely high speed avenues for space communications: optical & W-band waves. *8th ASMS/14th SPSC*, 5 September 2016.
5. Paraboni A, Buti M, Capsoni C, et al. Meteorology-driven optimum control of a multibeam antenna in satellite telecommunications. *IEEE Trans Antennas Propag*. FEBRUARY 2009;57(2):508-519.
6. Ippolito LJ. Satellite communications systems engineering: atmospheric effects, satellite link design and system performance. John Wiley & Sons, Ltd; 2008. ISBN: 9780470725276
7. Multibeam satellite communication system and Method and satellite payload for carrying out such a method, International Application Published under the patent cooperation treaty (PCT), WO 2014/001837 A1.
8. Riva C. Seasonal and diurnal variations of total attenuation measured with the ITALSAT satellite at Spino d'Adda at 18.7, 39.6 and 49.5 GHz. *Int J Satell Commun Netw*. 2004;22(4):449-476.
9. Ventouras S, Wrench CL, Callaghan SA. New thinking required to offset limitations imposed by V-band propagation. *19th AIAA Int. Comm. Sat. Sys. Conf*., Toulouse, France, 2001.
10. Barbaliscia F, Ravaioli G, Paraboni A. Characteristics of the spatial statistical dependence of rainfall rate over large areas. *IEEE Trans Antennas Propag*. 1992;40(1):8-12.

11. Bertorelli S, Paraboni A. Simulation of joint statistics of rain attenuation in multiple sites across wide areas using ITALSAT data. *IEEE Trans Antennas Propag*. Year: 2005;53(8):2611-2622.
12. Capsoni C, Castanet L, Gabellini P, et al. Use of space-time channel models and data for design and control of adaptive SatCom systems, *Proceedings of the 5th European Conference on Antennas and Propagation (EUCAP)*, Year: 2011, Pages: 3389–3392
13. Ventouras S, Crawford PS, Martellucci A. Definition of propagation elements for system design of broadband satellite systems in Ka and Q/V band. ESA/ESTEC Contract No 4000109354/13/NL/NR Final Report, February 2017.
14. Arbesser-Rastburg BR, Paraboni A. European research on Ka-band slant path propagation. *Proc IEEE*. 1997;85(6):843-852.
15. OPEX: Reference Book on Attenuation. *2nd Workshop of the Olympus propagation experimenters (OPEX), Doc*. ESA-ESTEC-WPP-083 volume 2, Noordwijk, The Netherlands, 1994.
16. Paraboni A, Riva C, Valbonesi L, Mauri M. Eight years of ITALSAT copolar attenuation statistics at Spino d'Adda. *Space Commun*. 2002;18:59-64.
17. Ventouras S, Callaghan SA, Wrench CL. Long-term statistics of tropospheric attenuation from the Ka/U band ITALSAT satellite experiment in the United Kingdom. *Radio Sci*. 2006;41(2):RS2007. https://doi.org/10.1029/2005RS003252
18. Davarian F. Ka-band propagation research using ACTS. *Int J Satell Commun*. 1996;14(3):267-281.
19. Lemorton J, Castanet L, Lacoste F, Van de Kamp MMJL, Riva C, Matricciani E, Fiebig UC. Development of propagation models for telecommunication satellite systems. ESA study No. 16865/03/NL/EC, ONERA Final report RF 4/07757 DEMR, September 2004.
20. ESA 17760/03/NL/JA. Characterisation and modelling of propagation effects in 20 to 50 GHz band, Politechnico di Milano, 2006.
21. Final Report 'Development of High order propagation models for Multimedia Satellite Communications Systems' Prime ONERA, ESA Contract 4000107135/12/NL/LVH, November 2016
22. Rossi T, De Sanctis M, Ruggieri M, et al. Satellite communication and propagation experiments through the Alphasat Q/V band Aldo Paraboni technology demonstration payload. *IEEE Aerosp Electron Syst Mag*. March 2016;31(3), part I of II):18-27. https://doi.org/10.1109/TAES.2016.150220
23. Vilhar A, Kelmendi A, Hrovat A, Kandus G. First year analysis of Alphasat Ka- and Q-band beacon measurements in Ljubljana, Slovenia. *Proc 22nd Ka and Broadband Conf, Cleveland (USA)*, October 17–20, 2016.
24. Hrovat A, Kandus G, Kuhar U, Kelmendi A, Vilhar A. A Ka-band satellite beacon receiver for propagation experiment. *Informacije MIDEM*. 2016;46(1):13-23.
25. Pek V, Fiser O. Atmospheric attenuation analysis using Aldo-Alphasat beacon signal in Prague. Proc. Marew 2017 conference, Brno, 2017.
26. Ventouras S, Davies PG, Norbury JR. OLYMPUS-based propagation measurements in Southern UK. *ICAP'95*, IEE Conf Pub 407, pp 27–31,1995
27. Woodroffe JM, Davies PG, Norbury JR. Combined OLYMPUS and ITALSAT propagation experiment in the UK, paper presented at Olympus Utilisation Conference, ESA, Seville, Spain 1993.
28. S3 Satcom Guide to small antenna tracking and Pointing – July 2009 – v1-1.pdf.
29. Agnew JL, Ventouras S. Meteorological measurements at Chilbolton Observatory, UK. *2nd Assembly of Alphasat Experimenters* in Oct 2015.
30. ITU-R Study Group 3 Fascicle 3M/FAS/8, The processing of tipping bucket rain gauge data for Study Group 3 experimental database, https://www.itu.int/en/ITU-R/study-groups/rsg3/Pages/fascicles.aspx
31. Agnew JL. A method for ongoing validation of profiling microwave radiometer water vapour products using radiosonde data. *Proceedings 9th ISTP conference*, University of L'Aquila, 2012.
32. Machado F, Fontán FP, Pastoriza V, Mariño P. The Ka- and Q-band Alphasat ground station in Vigo, in *2015 9th European Conference on Antennas and Propagation (EuCAP)*, Lisbon, 2015:1–4.
33. Machado F, Vilar E, Fontán FP, Pastoriza V, Mariño P. Easy-to-build satellite beacon receiver for propagation experimentation at millimeter bands. *Radioengineering*. Apr. 2014;23(1):154-163.
34. Rocha A. Propagation experiment at Ka band. *10th Ka and Broadband Communications Conference*, pp. 127–133, 2004.
35. Fiser O, Pek V, Brazda V, Schejbal V. Experiences with special Ka- and Q-band receivers for Alphasat signal monitoring in Prague, CZ. *Proc. of conf. Marew* 2017.
36. Nessel J, Gousetis G, Zemba M, Houts J. Design and preliminary results from Edinburgh, UK Alphasat Q-band propagation terminal. *In 22nd Ka and Broadband Communications Conference, Cleveland*, Ohio 2016, October.
37. Perez RO, Martellucci A, Graziani A. Description of the satellite propagation experiment exchange data format (SPEX v1.0), Ref. Number TEC-EEP/2014.50/ROP, Issue 1, Rev. 8, TN, 24/02/2017
38. Flávio J, Rocha A, Mota S, Jorge F. Alphasat experiment at Aveiro: data processing approach and experimental results, in European Conference on Antennas and Propagation, 2017:2376–2380.
39. ESA 4000109353/13/NL/NR, Data collection and processing system for the Alphasat TDP5 Ka/Q band propagation experiment, Final Report, May 2017.
40. Vilhar A, Kelmendi A, Hrovat A. Satellite propagation experiment in Ljubljana: beacon measurements at Ka-and Q-band in European Conference on Antennas and Propagation, 2017:3300–3304.
41. Jeannin N., Outeiral M., Castanet L., et al. Atmospheric channel simulator for the simulation of propagation impairments for Ka band data downlink, *The 8th European Conference on Antennas and Propagation (EuCAP* 2014*)*, Year: 2014, Pages: 3357–3361
42. Skamarock WC, Klemp JB, Dudhia J, Gill DO, Barker DM, Wang W, Powers JG. A description of the advanced research WRF Version 3. *NCAR Technical Notes* 2008; TN-475+STR.
43. Outeiral García M, Jeannin N, Féral L, Castanet L. Use of WRF model to characterize propagation effects in the troposphere. *7th European Conference on Antennas and Propagation*, Gothenburg, Sweden, 2013.

44. International Telecommunication Union (ITU), ITU-R Recommendation P.676-10, Attenuation due to clouds and fog, P series, Geneva, Switzerland, 2013.

45. International Telecommunication Union (ITU), ITU-R Recommendation P.840-6, Attenuation by atmospheric gases, P series, Geneva, Switzerland, 2013.

46. Quibus L, Luini L, Riva C, Vanhoenacker-Janvier D. Numerical weather prediction models for the estimate of clear-sky attenuation level in Alphasat beacon measurement. *12th European Conference on Antennas and Propagation*, London, U.K., 2018.

47. Fayon G, Féral L, Castanet L, Jeannin N, Boulanger X. Use of WRF to generate site diversity statistics in South of France. 32nd URSI GASS, 19–26 Aug. 2017, Montreal, Canada.

48. Matricciani E, Mauri M, Riva C. Relationship between scintillation and rain attenuation at 19.77 GHz. *Radio Sci*. March-April 1996;31(2):273-279.

49. Jeannin N, Boulanger X, Féral L, Castanet L, Lacoste F. Inter-annual variability, risk and confidence intervals associated with propagation statistics. Part I: theory of estimation. *Int J Satell Commun Netw*. 2014;32(5):407-421.

50. Boulanger X, Jeannin N, Féral L, Castanet L, Lacoste F, Carvalho F. Inter-annual variability, risk and confidence intervals associated with propagation statistics. Part II parameterization and applications. *Int J Satell Commun Netw*. 2014;32(5):423-441.

How to cite this article: Ventouras S, Martellucci A, Reeves R, et al. Assessment of spatial and temporal properties of Ka/Q band earth-space radio channel across Europe using Alphasat Aldo Paraboni payload. *Int J Satell Commun Network*. 2019;37:477–501. https://doi.org/10.1002/sat.1313